Desalination and Water Treatment
www.deswater.com

doi: 10.5004/dwt.2017.20147

62 (2017) 86–93
February

Variation of distillate flux in direct contact membrane distillation for water desalination

Ibrahim S. Al-Mutaz*, Abdulaziz S. Al-Motek, Irfan Wazeer

Chemical Engineering Department, College of Engineering, King Saud University, P.O. Box 800, Riyadh 11421, Saudi Arabia, email: almutaz@ksu.edu.sa

Received 29 June 2016; Accepted 29 July 2015

ABSTRACT

Membrane distillation is a thermally driven process that can be adapted effectively for water desalination. Vapor pressure gradient is the main driving force for mass transfer between hot feed and a colder distillate, making membrane distillation the only desalination membrane process that can maintain productivity almost independent of solution concentration. Other advantages of membrane distillation include low energy consumption and very high-quality distillate. Moreover, feed water to the membrane distillation does not require extensive pre-treatment like reverse osmosis. A steady state mathematical model of membrane distillation system is developed based on the basic laws of energy balance, mass balance and heat transfer equations with physical properties correlations. The objective of this work is to have a fundamental understanding of membrane distillation as a promising technology in desalination. The impact of important operating and design variables on the distillate flux in direct contact membrane distillation is studied in this work. The potential application of membrane distillation in desalination particularly will also be explored by developing a rigorous mathematical model of the process.

Keywords: Thermal desalination; Direct contact membrane distillation; DCMD; Flux estimation; Modeling

1. Introduction

Water is the most demanding global concern facing humanity, even though the earth contains about 1.4 × 10^9 m^3 of water. The percentage of saltwater is 97%, and the remaining 3% is freshwater [1,2]. 80% of that freshwater is frozen in the ice caps. Gulf Cooperation Council (GCC) countries are deserts with no permanent rivers or lakes and scanty rainfall. With the rapid growth in population, the demand for water is increasing. GCC countries depend on more than 80% of desalinated water as a primary source of drinking water [3]. The GCC countries produce 10,653,080 m^3/d of water, which is about half the world's total. There are around 90% of water desalination plants in Saudi Arabia ran on oil or natural gas as the source of energy, which is economically unsound. Desalination is an energy-intensive process, and many oil-producing countries are diverting their natural energy resources (oil and gas) to the local production of electricity, water desalination and transportation instead of exporting these resources to increase national income [4].

The desalination methods of water can be divided into two broad sectors: (1) thermal processes and (2) membrane processes [5,6]. Thermal desalination processes are further divided into three main categories: multi-stage flash desalination (MSF), multiple-effect desalination (MED) and vapor compression (VC). Imperative types of membrane distillation (MD) process are reverse osmosis (RO), electrodialysis (ED), nanofiltration (NF) and MD. RO process uses a semipermeable membrane to desalinate water. Currently, the worldwide market share for RO is around 50%. NF is a membrane filtration based method that uses nanometer-sized cylindrical through pores that pass through the membrane at a 90°.

MD is thermal membrane separation process, which can be used for water desalination, but also for recycling. The main difference between MD and other membrane separation

---

* Corresponding author.

process is the driving force of mass transfer [7]. MD can produce fresh water at low temperature. Additionally, high salt rejection can be achieved. This technology can work near to saturated concentration. It works at low hydrostatic pressure and requires less pre-treatment cost as compared with RO process. MD is less sensitive to feed characteristics (e.g., pH and total dissolved solids (TDS)). Low-grade thermal energy is the major energy requirement for MD system. Over the last two decades, various work has been published concerning modeling of MD system.

Martínez et al. [8] characterized three hydrophobic porous membranes used in MD. They modeled and evaluated water vapor permeability by assuming the common model of cylindrical capillaries for the membrane. They used flux equations, which include both diffusive and viscous mechanisms for transport in the gas phase in pores. Cath et al. [9] performed an experimental study of desalination using direct contact MD (DCMD). They developed new configurations with reduced temperature polarization effects. Upon comparison with previous results, they concluded that mass transport of water vapors was substantially improved by using their configuration with salt rejection greater than 99.9%. Close and Sørensen [10] studied the mathematical model of MD for desalination to determine the optimal operation and design of MD system. Excellent agreement was found between the results given by the model and actual experiments presented in the literature. They claimed that their model was able to provide an explanation for any conflicting results in the literature regarding the effect of the variables on the flux. Onsekizoglu [11] discussed the theoretical aspects and the relevant mathematics related to water transport mechanism in MD. Moreover, he discussed variant MD system operating at a lower temperature. He suggested that model configuration together with contact angle and membrane wettability should be considered for selecting a membrane. Camacho et al. [12] developed a general review of the fundamental heat and mass transfer processes in MD for possible modeling of MD process. They considered the recent advances in membrane technology, model configurations and the applications and economics of MD. They also identified areas that may lead to technological improvements in MD as well as the application characteristics required for commercial deployment. In this paper, a steady-state mathematical model of MD system is developed. Also, all aspects of the design procedure for a MD system are considered. DCMD has been modeled as a potential process for seawater desalination.

2. Configurations of membrane distillation

The MD has two modules: tubular module, and plate and frame module [13]. The tubular module consists of hollow fiber membrane mainly prepared from polypropylene (PP), polyvinylidene fluoride (PVDF), and PVDF-polytetrafluoroethylene (PTFE) composite materials. The plate and frame module includes flat sheet membrane largely prepared from PP, PTFE, and PVDF.

In MD, an aqueous feed solution is brought and heated on one side to the surface of a hydrophobic and porous membrane. This membrane acts as a physical interface between hot and cold streams. Various procedures have been engaged in imposing the vapor pressure difference across the membrane matrix. In each configuration of MD, feed water to be desalted directly contacts the hot side of a membrane.

MD has four configurations: (i) air gap MD (AGMD), (ii) vacuum MD (VMD), (iii) sweep gas MD (SGMD), and (iv) DCMD. In AGMD, only the feed aqueous solution is in direct contact with the membrane. In this configuration, the evaporated volatile molecules condense over a cold surface inside the membrane module after passing both the membrane pores and the air gap. In VMD, a vacuum is applied to the permeate side of the membrane module using a vacuum pump. The saturation pressure of volatile molecules to be isolated from the feed solution is higher than the applied vacuum pressure. Therefore, condensation of volatile molecules takes place outside of the membrane module. SGWD is similar to the AGMD; in both configurations, permeate is collected externally. In this arrangement, the evaporated volatile molecules cross both the membrane pores and the air gap to condense finally over a cold surface inside the membrane module. In DCMD configuration, both hot and cold aqueous streams are in direct contact with the membrane on both sides. DCMD has been considered as the most appropriate MD configuration and module for water desalination in this work based on a comprehensive literature survey of MD processes. DCMD is best suited for the desalination applications where water is the permeating flux, and this configuration does not require an external condenser [13]. Various salt concentrations can be treated using DCMD setup, and it operates at near-atmospheric pressure since it is not subjected to the osmotic pressure-driven limitations of RO. DCMD provides complete rejection of nonvolatile such as ions, salts, cells and organic nonvolatile. Furthermore, this arrangement needs less mechanical strengths for the membrane as compared with RO. Table 1 lists the characteristics of membranes employed for water desalination.

3. Process description

The original idea of MD was introduced by DCMD. MD has mass and heat transfer both in the same direction from hot side to the cold side. Fig. 1 shows a simplified diagram of DCMD process. Both the feed and permeate aqueous solutions are circulated tangentially to the membrane surfaces by means of circulating pumps and stirred inside the membrane cell using a magnetic stirrer. In this arrangement, the transmembrane temperature difference induces a vapor pressure difference. Consequently, volatile molecules evaporate at the hot liquid/vapor interface, cross the membrane pores in vapor phase and condense in the cold liquid/vapor interface inside the membrane module. The temperature of the feed decreases along feed side until reaches the boundary layer to become boundary temperature. Water evaporates and transports through the hydrophobic membrane pores. Heat is conducted through the membrane to cold side. In the permeate side, cold flow temperature increases across the permeate side boundary layer to boundary temperature at membrane surface. Water vapor condenses and gains heat from feed side. The driving force is the vapor pressure difference between feed temperatures at membrane surface and permeate temperature at membrane surface, which is less than vapor pressure difference between feed and permeate temperature, and this

Table 1
Characteristics of some membranes used for water desalination [9,14,15]

Membrane	Manufacturer	Material	δ (μm)[a]	ε[a]	τ[a]	*dp*[a] (μm)	Conductivity (W/m K)
TF200	Gelman, USA	PTFE/PP	178	0.80	1.59	0.20	0.031
TF450	Gelman, USA	PTFE/PP	178	0.80	1.44	0.45	0.027
GVHP	Millipore, Germany	PVDF	110	0.75	2.14	0.22	0.041
PTFE0.2	Millipore, Germany	PTFE	175	0.70	NA	0.20	NA
PTFE0.5	Millipore, Germany	PTFE	175	0.85	NA	0.50	NA
PS22	NA	PP	150	0.70	NA	0.22	NA
TS22	NA	PTFE	175	0.70	NA	0.22	NA

[a] Symbols: δ – membrane thickness; ε – porosity; τ – membrane tortuosity and *dp* – pore size.

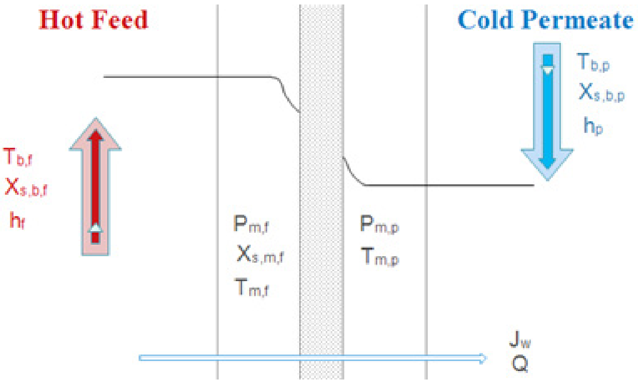

Fig. 1. A simplified diagram of DCMD process.

phenomenon is called temperature polarization. Therefore, mass transfer takes place when the hot feed vaporizes from the liquid/gas interface, and the vapor is moved across membrane pores from hot side to cold side by vapor pressure difference. Eventually, the condensation of vapor takes place on the cold side (permeate). The controlling factors of mass transfer in MD process are vapor pressure difference and permeability.

4. Mathematical modeling

The following assumptions were used to solve DCMD mathematical equations:

- Steady-state operation.
- Heat transfer by conduction is negligible for nonsport thin membrane.
- The kinetic effects at the vapor-liquid interface are negligible.
- Pore radius is uniform for the membrane.

The mass transfer mechanism in the membrane pores is governed by three mechanisms: (1) Knudsen diffusion (K), (2) Poiseuille flow (P) and (3) molecular diffusion (M) or a combination between any of these mechanisms, which is known as transition mechanism. In the DCMD, the component in the pores is vapor–air mixture, and the mass transfer mechanism is M–K [16], which can be given by:

$$J_w = B_w(p_{m,f} - p_{m,p}) \tag{1}$$

where B_w is the membrane permeability, and $p_{m,f}$ and $p_{m,p}$ are partial vapor pressures at membrane surface in both feed and permeate sides, respectively. By using Antoine equation, the above equation can be rewritten to be represented in term of temperature difference across the membrane:

$$J_w = B_w\left(\frac{dp}{dT}\right)_{T_m}(T_{m,f} - T_{m,p}) \tag{2}$$

where $T_{m,f}$ and $T_{m,p}$ are membrane temperatures at feed and permeate sides, respectively. The mass transport mechanism in the membrane pores is governed by the free mean path of the transported water vapor inside membrane pore. The Knudsen number (*Kn*) is used to indicate the dominant mass transfer mechanism in the pores:

$$Kn = \lambda / d_p \tag{3}$$

where d_p is the membrane pore size, and λ is the free mean path of water molecules in vapor phase, which can be evaluated by:

$$\lambda = \frac{k_B T}{\sqrt{2}P_m(2.641\times10^{-10})^2} \tag{4}$$

where k_B is the Boltzmann constant; P_m is the mean pressure and T is the absolute temperature.

Knudsen type of flow is responsible for the mass transfer through the membrane pore when the mean free path of the transported water molecules in vapor phase is greater than the membrane pore size, i.e., $Kn > 10$ or $dp < 0.1\ \lambda$. The molecule-pore wall collisions are dominant over the molecule-molecule collisions. B_w can be given by:

$$B_w = \frac{2\pi}{3RT_m}\left(\frac{8RT_m}{\pi M_w}\right)^{1/2}\frac{r^3}{\tau\delta} \tag{5}$$

where r is pore radius in the membrane; τ is membrane tortuosity; δ is membrane thickness; M_w is molecular weight and T_m is mean temperature.

Molecular diffusion type of flow is responsible for the mass transport in continuum region caused by the stagnant air trapped within each membrane pore due to the low solubility of air in water ($Kn < 0.01$ or $dp > 100\ \lambda$). B_w can be given by:

$$B_w = \frac{\pi PDr^2}{RTp_a\tau\delta} \tag{6}$$

where D is the diffusion coefficient; P is total pressure inside the membrane pore and P_a is the air pressure in the membrane pore. The PD can be calculated as:

$$PD = 1.895\times10^{-5}\times T^{2.072} \tag{7}$$

The water vapor transport takes place via a combined Knudsen/ordinary diffusion mechanism when the calculated λ values are similar to the pore size of the membranes used in DCMD. In transition region, $0.01 < Kn < 10$ (i.e., $0.1\ \lambda < dp < 100\ \lambda$). In that situation, the water vapor permeability of the membrane can be written as:

$$B_w = \frac{1}{RT_m\delta}\left(\frac{3\tau}{2\varepsilon r}\left(\frac{\pi M_w}{8RT_m}\right)^{0.5} + \frac{p_a\tau}{\varepsilon PD}\right)^{-1} \tag{8}$$

where r is pore radius in the membrane; τ is membrane tortuosity; δ is membrane thickness; M_w is molecular weight and T_m is mean temperature.

$(dP/dT)_{Tm}$ is obtained from Clausius Clapeyron and can be expressed as:

$$\left(\frac{dp}{dT}\right)_{T_m} = \frac{\Delta H_{v,m}}{RT_m^2}\exp\left(23.238 - \frac{3841}{T_m - 45}\right) \tag{9}$$

Then the flux can be written as:

$$J_w = B_w\left(\frac{dp}{dT}\right)_{T_m}\times[(T_{m,f} - T_{m,p}) - \Delta T_o](1 - x_{s,m,f}) \tag{10}$$

where ΔT_o is:

$$\Delta T_o = \frac{RT_m^2}{\Delta H_{v,m}}\left(\frac{x_{s,b,f} - x_{s,b,p}}{1 - x_{s,m,f}}\right) \tag{11}$$

where $x_{s,m,f}$ and $x_{s,m,p}$ are mole fraction of solute at membrane surface in the feed and permeate sides, respectively.

$\Delta H_{v,w}$ is the latent heat of vaporization, and it can be written as:

$$\Delta H_{v,m} = 1.7535T_m + 2024.3 \tag{12}$$

As can be seen in Eq. 8, water flux depends on heat transfer between the feed and the membrane ($T_{m,f} - T_{m,p}$). These temperatures are implicitly involved in the heat balance equations. Therefore, heat transfer in the MD will be considered.

Heat is transferred from the hot feed across membrane as sensible heat and latent heat, and then heat transferred from the bulk flow of the feed to boundary layer by convection. The sensible heat is conducted through the membrane to the cold side, and the latent heat of vaporization is carried by the water vapor, which is evaporated at the interface between the hot stream and membrane pores and is condensed at the interface between the pores and cold stream.

Heat transfer by convection in the feed boundary layer is governed by:

$$Q_f = h_f(T_{b,f} - T_{m,f}) \tag{13}$$

where h_f is the heat transfer convection coefficient on the hot side, and $T_{b,f}$ and $T_{m,f}$ are feed and boundary layer temperatures on the feed side, respectively.

Heat transfer by conduction across membrane is given by:

$$Q_m = \frac{K_m}{\delta}(T_{m,f} - T_{m,p}) + J_w\Delta H_{v,w} \tag{14}$$

where K_m is the thermal conductivity of the membrane; δ is the membrane thickness; J_w is the permeate flux; $\Delta H_{v,w}$ is the latent heat of vaporization, and $T_{f,m}$ and $T_{p,m}$ are feed and permeate boundary layer temperatures, respectively. The Isostress model defined K_m as:

$$K_m = \left[\frac{\varepsilon}{K_g} + \frac{(1-\varepsilon)}{K_p}\right]^{-1} \tag{15}$$

where K_p is the thermal conductivity of membrane material, and K_g is the thermal conductivity of gas that filling the pores. ε is porosity, which is defined as a fraction of voids over the total volume.

Heat transfer by convection in the permeate boundary layer can be written as:

$$Q_p = h_p(T_{m,p} - T_{b,p}) \tag{16}$$

where h_p is heat transfer coefficients in the permeate boundary layer.

Heat transfer coefficients for both feed and permeate side (h_f and h_p) can be obtained by means of Nusselt numbers given by [17]:

$$h_i = \frac{Nu_i k_i}{d_h}, \quad \text{where } i = f, p \tag{17}$$

where h is the heat transfer coefficient; d_h is the hydraulic diameter and k is the thermal conductivity.

For turbulent flow ($2{,}500 < Re < 1.25 \times 10^5$), the following empirical correlation can be used [18,19]:

$$Nu = 0.023\,Re^{0.8}Pr^{0.33}\left(\frac{\mu}{\mu_s}\right)^{0.14} \tag{18}$$

For laminar flow ($Re < 2{,}100$), the following correlation can be used [19]:

$$Nu = 1.86\left(Re\,Pr\frac{d_h}{L}\right)^{0.33} \tag{19}$$

In Eq. (19), L is the channel length, and Pr and Re are the Prandtl and Reynolds numbers, respectively:

$$Re = \frac{d_h v \rho}{\mu}, \quad Pr = \frac{c_p \mu}{k} \tag{20}$$

where v, ρ, μ, c_p and k are the average velocity, the density, the viscosity, the specific heat and the thermal conductivity of the liquid, respectively.

The overall heat transfer flux through the membrane at steady state is:

$$Q = Q_f = Q_m = Q_p \tag{21}$$

By substituting expression of Q_f, Q_m and Q_p:

$$\begin{aligned} h_f(T_{b,f} - T_{f,m}) &= \frac{K_m}{\delta}(T_{f,m} - T_{p,m}) + J_w \Delta H_{v,w} \\ &= h_p(T_{p,m} - T_{b,p}) \end{aligned} \tag{22}$$

The overall heat transfer flux can be written as:

$$Q = U(T_{b,f} - T_{b,p}) \tag{23}$$

where U is the overall heat transfer resistance, and $T_{b,f}$ and $T_{b,p}$ are feed and permeate bulk temperatures, respectively.

Heat transfer resistance in the DCMD is presented in Fig. 2. In this figure, R_f is thermal resistance of hot feed, R_m is thermal resistance of membrane, which is combination of R_c is thermal resistance of whole membrane and R_v is thermal resistance of vapor, and R_p is thermal resistance of cold permeate. To find overall heat transfer resistance, first the membrane thermal resistance shall be evaluated. Inside membrane, there are two parallel thermal resistances. One of them is thermal resistance of membrane material and gas filled pores h_m. The other is vapor heat transfer h_v, which can be represented as:

$$\frac{1}{R_m} = \frac{1}{K_m/\delta} + \frac{1}{J_w \Delta H_{v,m}/\Delta H_m} \tag{24}$$

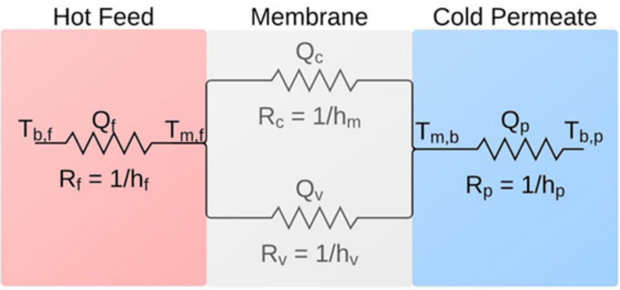

Fig. 2. Heat transfer resistance in DCMD.

Since all thermal resistances are in series, they can be written as:

$$\frac{1}{U} = R_f + R_m + R_p \tag{25}$$

$$\frac{1}{U} = \frac{1}{h_f} + \frac{1}{K_m/\delta} + \frac{1}{J_w \Delta H_{v,w}/\Delta H_m} + \frac{1}{h_p} \tag{26}$$

The overall heat transfer resistance is then:

$$U = \left[\frac{1}{h_f} + \frac{1}{\dfrac{K_m}{\delta} + \dfrac{J_w \Delta H_{v,w}}{\Delta T_m}} + \frac{1}{h_p}\right]^{-1} \tag{27}$$

where

$$\Delta T_m = T_{f,m} - T_{p,m} \tag{28}$$

where $T_{m,f}$ and $T_{m,p}$ are the temperatures at the feed membrane and membrane permeate interfaces, respectively. These temperatures can be obtained by solving Eq. (17) and can be represented as:

$$T_{m,f} = \frac{\dfrac{K_m}{\delta}\left(T_{b,p} + \dfrac{h_f}{h_p}T_{b,f}\right) + h_f T_{b,f} - J_w \Delta H_{v,w}}{\dfrac{K_m}{\delta} + h_f\left(1 + \dfrac{K_m}{\delta h_p}\right)} \tag{29}$$

$$T_{m,p} = \frac{\dfrac{K_m}{\delta}\left(T_{b,f} + \dfrac{h_p}{h_f}T_{b,p}\right) + h_p T_{b,p} - J_w \Delta H_{v,w}}{\dfrac{K_m}{\delta} + h_p\left(1 + \dfrac{K_m}{\delta h_f}\right)} \tag{30}$$

5. Solution algorithm

From the previous equations, the following procedure is followed to find the rate of water flux:

1. The permeate flux can be given as a function of the bulk vapor pressure difference. Eq. (1) can be rewritten for an overall vapor pressure difference as:

   $$J_w = B_w \Delta P_w \tag{31}$$

   where P_w can be given as:

   $$P_w(x,T) = P_w^o(T)\,a_w(x) \tag{32}$$

   where P_w^o can be given by Antoine equation, and a_w is water activity.
2. For the first guess, the balk permeate temperature, $T_{b,p}$ will be assumed. By using the bulk feed temperature, $T_{b,f}$, mean membrane temperature, T_m, is found by:

   $$T_m = \frac{T_{b,f} + T_{b,p}}{2} \tag{33}$$

3. Evaluate the free mean path of water molecules in vapor phases λ from Eq. (4).
4. Using free mean path of water molecules in vapor phases λ from previous step to evaluate the Knudsen number (Kn).
5. After indicating the dominant mass transfer mechanism in the pores use T_m from step 2 with the appropriate equation of B_w between Eqs. (5), (6) and (8).
6. Using B_w from previous step in Eq. (31) to evaluate global water flux J_w.
7. Evaluate $\Delta H_{v,w}$ from Eq. (12) using T_m from step 2.
8. Evaluate $(dP/dT)_{Tm}$ from Eq. (9) using value of $\Delta H_{v,w}$ from previous step and value of T_m from step 2.
9. Evaluate value of ΔT_o from Eq. (11) using value of $\Delta H_{v,w}$ from step 7 and value of T_m from step 2.
10. Using water flux value from step 4 with Eqs. (29) and (30) to determine $T_{f,m}$ and $T_{p,m}$, where K_m and δ values in Table 1 depending on type of membrane are chosen. Where the latent heat of vaporization $\Delta H_{v,w}$ evaluated in step 5 and value of T_m evaluated in step 2.
11. Evaluate value of water flux from Eq. (10) using value of B_w from step 5, from step 8 use value of $(dP/dT)_{Tm}$, values of $T_{f,m}$ and $T_{p,m}$ from step 10, and value of ΔT_o from step 9.
12. Comparing value of water flux from step 6 with step 11.
13. If value not matched, go to step 2 and reassume bulk permeate temperature.

6. Results and discussion

The aim of the presented model is to study the flux variation in DCMD system for water desalination. The commercial membrane used in DCMD model is TF200. The equations for DCMID model are highly nonlinear; hence, an iterative solution for direct substitution is suggested to solve these equations simultaneously. In this regard, a MATLAB code has been developed to solve the model equations. The obtained results were compared with the experimental work of [9,20,21], and good agreement was achieved.

The effect of feed temperature on water flux is demonstrated in Fig. 3. The water flux through the membrane increased linearly with temperature, which is due to the substantial influence of the membrane thickness over the thermodynamic effects. As can been seen in Table 1, TF 200 is substantially thicker than other membranes. The similar results between water flux and feed temperature were reported by Cath et al. [9]. Permeability coefficient in MD is a function of the reciprocal of the membrane thickness [18]:

$$N \propto \frac{r^a \varepsilon}{\tau\delta} \tag{34}$$

where N is the permeability coefficient; ε the membrane porosity; r the membrane pore size; α a diffusion parameter; τ the pore tortuosity and δ is the thickness of the membrane.

Fig. 4 depicts the variation of temperature polarization (θ) with feed temperature. Temperature polarization decreases with the rise in feed bulk temperature of DCMD process. Cath et al. [9] also revealed that the optimal design of membrane module and configuration of the MD system could result in the reduction of permeability obstructions and temperature polarization in the DCMD of salt solutions. Martínez-Díez and Vázquez-González reported that the formation of polarization layers on either side of membrane reduce water permeation in DCMD [21]. They also stated that the temperature polarization has a significant influence on water flux.

The change in vapor pressure difference across the membrane with feed temperature is shown in Fig. 5. This is a

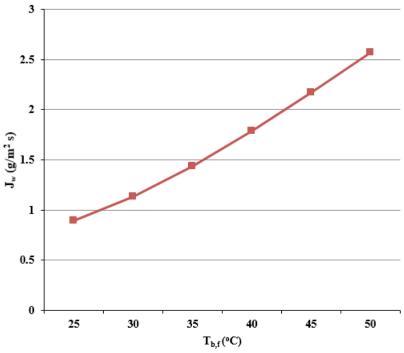

Fig. 3. Variation of water flux vs. feed temperature ($T_{b,f}$) in DCMID.

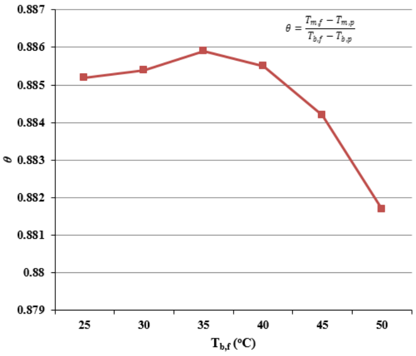

Fig. 4. Effect of bulk feed temperature on temperature polarization.

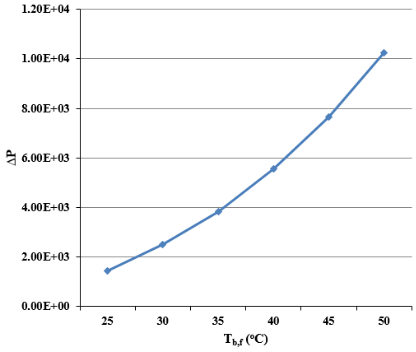

Fig. 5. Feed temperature ($T_{b,f}$) vs. driving force (ΔP) in DCMD.

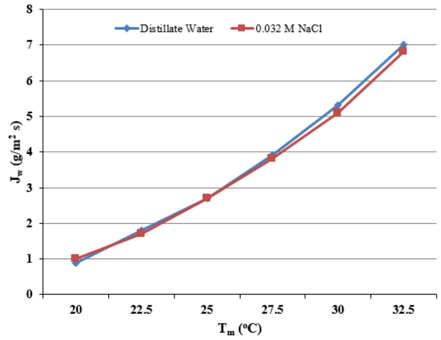

Fig. 6. Water flux vs. mean temperature (T_m) for 0.032 M NaCl solution and distillate water.

normal phenomenon since the change in vapor pressure is directly proportional to the feed temperature.

The effect of mean temperature (T_m) on water flux for 0.032 M NaCl solution and distillate water in DCMD process is displayed in Fig. 6. There is no significant change in the water flux for saline water and distillate water, which is one of the most noteworthy advantages of the DCMD process for desalination. Cath et al. [9] also demonstrated that the increase in salt concentration minimally decreases the vapor pressure of water and therefore only marginally decreases the driving force for mass transfer. In RO, the driving force for mass transport decreases significantly due to increasing in feed salt concentration, and also, the passage of salt through the membrane increases.

Fig. 7 depicts the effect of increasing permeate temperature for DCMD process. As perceived from the figure, the flux prediction reduces with increase in the permeate temperature. The similar trend was reported by [20]. Because, as the permeate temperature increases, there is a decrease in the temperature difference between the feed and the permeate chambers, which leads to the reduction of water flux.

The cost of energy supply for heating the feed water in DCMD desalination plant is negligible if it is combined with a power plant or any other waste heat source. Geothermal or renewable solar energy could also be used to heat the feed water DCMD desalination plant [22,23]. In DCMD process, two pumps are required for the operation: one for the feed water and one for the coolant water. However, this process does not require high pressure as compared with RO, and low-pressure pumps are cheaper in both operating and capital cost. The major concern regarding the DCMD treatment process is cleaning of the membrane [24]. Most of the MD membranes are made of chemically resistant polymers, which can tolerate chlorine and other oxidizing agents.

7. Conclusions

This work presents a useful and precise mathematical model describing the DCMD desalination system. MATLAB code was developed and utilized to solve the mathematical model of the DCMD system. The analysis is based on the core concepts of heat and mass balance to study the flux variations in DCMD. This paper illustrates that the simulation model is an efficient tool to design DCMD system with any desired capacity. Good agreement is obtained between model data and published data. Parametric study of DCMD system was also executed. The presented model was tested on the effect of permeate temperature, feed temperature, feed salinity and the mean temperature. Results have revealed that higher fluxes can be attained compared with the old-fashioned mode of DCMD process at relatively low temperatures. Results have also shown that the salt concentration in the feed solution does not affect the operation of MD process. The developed model can predict the vapor flux (permeability) and membrane surface temperatures simultaneously, taking into consideration the effects of the applied membrane physical properties.

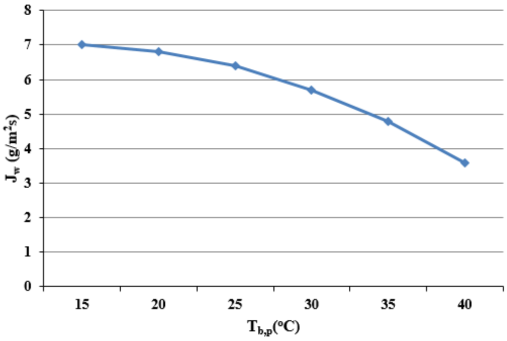

Fig. 7. Water flux vs. permeate bulk temperature ($T_{b,p}$) in DCMD.

Acknowledgment

The authors would like to extend their sincere appreciation to the Deanship of Scientific Research at King Saud University for its funding of this research through the Research Group Project number RGP-224.

References

[1] I.S. Al-Mutaz, I. Wazeer, Economic optimization of the number of effects for the multieffect desalination plant, Desal. Wat. Treat., 56 (2015) 2269–2275.
[2] S.A. Kalogirou, Seawater desalination using renewable energy sources, Prog. Energy Combust. Sci., 31 (2005) 242–281.
[3] I.S. Al-Mutaz, I. Wazeer, Current status and future directions of MED-TVC desalination technology, Desal. Wat. Treat., 55 (2015) 1–9.

[4] H. Fath, A. Sadik, T. Mezher, Present and future trend in the production and energy consumption of desalinated water in GCC Countries, Int. J. Therm. Environ. Eng., 5 (2013) 155–165.

[5] I.S. Al-Mutaz, I. Wazeer, Comparative performance evaluation of conventional multi-effect evaporation desalination processes, Appl. Therm. Eng., 73 (2014) 1194–1203.

[6] I.S. Al-Mutaz, I. Wazeer, Development of a steady-state mathematical model for MEE-TVC desalination plants, Desalination, 351 (2014) 9–18.

[7] M. El-Bourawi, Z. Ding, R. Ma, M. Khayet, A framework for better understanding membrane distillation separation process, J. Membr. Sci., 285 (2006) 4–29.

[8] L. Martínez, F.J. Florido-Díaz, A. Hernandez, P. Pradanos, Characterisation of three hydrophobic porous membranes used in membrane distillation: modelling and evaluation of their water vapour permeabilities, J. Membr. Sci., 203 (2002) 15–27.

[9] T.Y. Cath, V.D. Adams, A.E. Childress, Experimental study of desalination using direct contact membrane distillation: a new approach to flux enhancement, J. Membr. Sci., 228 (2004) 5–16.

[10] E. Close, E. Sørensen, Modelling of Direct Contact Membrane Distillation for Desalination, 20th European Symposium on Computer Aided Process Engineering, S. Pierucci, G.B. Ferraris, Eds., Elsevier, Naples, Vol. 28, 2010, pp. 649–654.

[11] P. Onsekizoglu, Membrane Distillation: Principle, Advances, Limitations and Future Prospects in Food Industry, S. Zereshki, Ed., Distillation - Advances from Modeling to Applications, InTech, Rijeka, Croatia, 2012, pp. 233–266.

[12] L.M. Camacho, L. Dumée, J. Zhang, J. Li, M. Duke, J. Gomez, S. Gray, Advances in membrane distillation for water desalination and purification applications, Water, 5 (2013) 94–196.

[13] A. Alklaibi, N. Lior, Membrane-distillation desalination: status and potential, Desalination, 171 (2005) 111–131.

[14] S.T. Hsu, K.T. Cheng, J.S. Chiou, Seawater desalination by direct contact membrane distillation, Desalination, 143 (2002) 279–287.

[15] M. Khayet, A.O. Imdakm, T. Matsuura, Monte Carlo simulation and experimental heat and mass transfer in direct contact membrane distillation, Int. J. Heat Mass Transfer, 53 (2010) 1249–1259.

[16] J. Zhang, Theoretical and Experimental Investigation of Membrane Distillation, Ph.D. Thesis, Victoria University, Australia, 2011.

[17] A. Alkhudhiri, N. Darwish, N. Hilal, Membrane distillation: a comprehensive review, Desalination, 287 (2012) 2–18.

[18] K.W. Lawson, D.R. Lloyd, Membrane distillation, J. Membr. Sci., 124 (1997) 1–25.

[19] S. Srisurichan, R. Jiraratananon, A. Fane, Mass transfer mechanisms and transport resistances in direct contact membrane distillation process, J. Membr. Sci., 277 (2006) 186–194.

[20] D.U. Lawal, A.E. Khalifa, Flux prediction in direct contact membrane distillation, Int. J. Mater. Mech. Manuf., 2 (2014) 302–308.

[21] L. Martínez-Díez, M.I. Vázquez-González, Temperature and concentration polarization in membrane distillation of aqueous salt solutions, J. Membr. Sci., 156 (1999) 265–273.

[22] F. Banat, R. Jumah, M. Garaibeh, Exploitation of solar energy collected by solar stills for desalination by membrane distillation, Renew. Energy, 25 (2002) 293–305.

[23] P. Hogan, A. Fane, G. Morrison, Desalination by solar heated membrane distillation, Desalination, 81 (1991) 81–90.

[24] J. Glater, S.k. Hong, M. Elimelech, The search for a chlorine-resistant reverse osmosis membrane, Desalination, 95 (1994) 325–345.